Int. J. Advanced Design and Manufacturing Technology, 2023, Vol. 16, No. 4, pp. 9-22

DOI: 10.30486/admt.2024.1980467.1402 *ISSN: 2252-0406* *https://admt.isfahan.iau.ir*

Simulation and Dynamic-Thermal Analysis of Ceramic Disc and Brake Pad for Optimization by Finite Element Method

Navvab Gholami, Ahmad Afsari *, Seyed Mohammad Reza Nazemosadat

Department of Mechanical Engineering, Shiraz Branch, Islamic Azad University, Shiraz, Iran
E-mail: Ah.Afsari1338@iau.ac.ir
*Corresponding author

Mohammad Javad Afsari

Department of Computer Engineering, University of Tehran, Tehran, Iran

Received: 17 February 2023, Revised: 14 December 2023, Accepted: 17 December 2023

Abstract: The braking system in automotives directly deals with the issue of safety, and as a result, it is essential to pay attention to this matter. One of the materials used to make disc and brake pads in disc brakes is ceramic material. This research aims to simulate and analyze the dynamic-thermal ceramic brake disc during the braking operation using the finite element method. Currently, the conventional brake disc is used in the Peugeot 206 automotive (domestic production), which has low efficiency in terms of life, wear, etc. Therefore, in this research, considering the significant production of Peugeot 206 automotive in the country, the disc and brake pads of this automotive have been selected, which were first modelled by Catia software, and after transferring the model to Abaqus software and defining the types of ceramics, Cast iron was analyzed by finite element method. The results of the Peugeot 206 ceramic brake disc and pad analysis were compared with the results of the standard (cast iron) discs in this automotive. The results showed that the maximum Von-Mises stress in the ceramic disc was 260.7 MPa, while the maximum Von-Mises stress in the cast iron disc was 293.3 MPa. The amount of heat produced in the ceramic disc during the braking action in 4 seconds was almost 84% less than the cast iron disc in the same period. Also, the results showed that the ceramic disc has a higher safety factor (1.98) than the cast iron disc (1.45).

Keywords: Brake Disc, Ceramic Materials, Finite Elements, Modeling, Pads

Biographical notes: Navvab Gholami graduated with a MSc degree in Mechanical Engineering from Islamic Azad University, Shiraz branch in 2022. **Ahmad Afsari** is an associate professor of Mechanical Engineering at Islamic Azad University, Shiraz branch. He received his PhD from the Indian Institute of Technology - Delhi, India in 1998. His speciality is in manufacturing and production methods (welding, casting, shaping and machining) and also precision measurement systems. **Seyed Mohammad Reza Nazemosadat** is an assistant professor of Mechanical Engineering at Islamic Azad University, Shiraz branch. He received his PhD in Mechanical Engineering of Biosystems from Shahrekord University in 2022. His current research is in the field of agricultural machinery and automotive design, FEM, chassis reliability analysis and optimization. **Mohammad Javad Afsari** is a computer engineering undergraduate student at the University of Tehran. His expertise is in the field of artificial intelligence and he cooperates with knowledge-based companies in this field.

Research paper

1 INTRODUCTION

As the most vital safety system in automotive, the brake has an important task; that's why from the past until now, it has witnessed the progress, evolution, and emergence of various innovations in automotive brake systems. Today, unlike in the past, brakes are responsible for slowing down and stopping the automotive and play a vital role in the automotive's steering. Now the question arises of how to improve the braking system in automotives and whether the materials that make up the parts of the braking system in automotives affect their improvement. Innovation in producing components such as pads and brake discs improved the braking and thus increased the automotive's safety. Ceramics are among the materials used in the production of brake pads and discs for modern automotives, which improve the braking power of automotives and increase their lifespan due to better heat transfer than cast iron and a higher friction coefficient [1].

Structurally, the brake system installed in the automotive can be divided into three general categories: wire brakes, hydraulic brakes, and pneumatic brakes. The handbrake, also known as the parking brake, is one of the wire brakes. A hand brake is used to keep a stopped automotive stable. In this case, the engine may be on or off. The handbrake must have the necessary power to keep the automotive stationary and be able to keep the automotive stationary on an incline of 30 degrees. A hydraulic brake is a type of hydraulic system that transfers the force of the brake pedal to the wheels. The components of the hydraulic brake system include the main cylinder, booster, combination valve, wheel cylinders, and mechanisms acting on the wheels. Pneumatic brake systems were first introduced in the railway industry of the United States of America by George Westinghouse in 1869 [2]. Later, trucks, buses, and even light trucks were used. The operation of the pneumatic brake is such that the ends of the brake shoes are connected to an S-shaped part. During braking, compressed air enters the air chamber and moves the transmission rod, causing the S-shaped part to rotate, and the shoes move and come into contact with the wheel bowl. It reduces the speed and eventually stops the wheels [3].

Based on the mechanisms acting on the wheel, the brake is divided into two categories, the drum, and the disc mechanism. In drum brakes, the brake drum is connected to the wheel and rotates with it, and two crescent-shaped iron shoes on which the brake pads are pressed are installed on the floor. In the typical case, when the automotive does not need to brake, they are adjusted so that there is a small distance between the brake drum and the pads of the shoes. When the driver presses the brake pedal, the oil pressure in the master cylinder increases. The internal pistons of the wheel cylinder move away from each other due to the oil pressure and move the brake shoes towards the brake drum. As a result of the force coming from the pad on the brake drum, the friction force between the drum and the pad is created, resulting in negative acceleration in the wheels and stopping them. An example of a brake with a drum mechanism can be seen in Fig. 1-b.

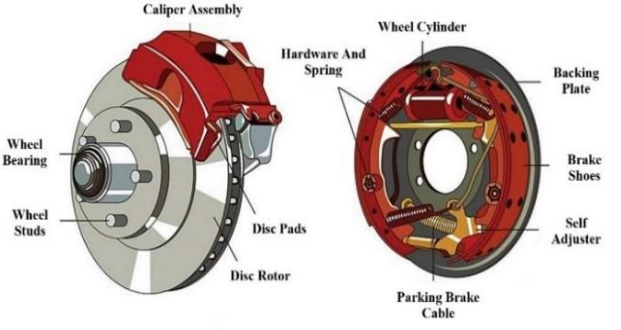

(a) **(b)**

Fig. 1 (a): Disc brake, and (b): Drum brake.

In an automotive disc brake, when the brake pedal is depressed, the push rod applies pressure to the master cylinder piston, allowing the return spring to push into the master cylinder bore, which creates pressure in the reservoir. A pellet of the oil fluid inside the reservoir allows it to enter the brake pipes, and a secondary bead ensures that oil does not flow back the other way. The oil enters the cylinder hole of the caliper set through the brake hoses and pushes the pistons of the caliper set that are connected to the pad forward causing the pad to contact the disc, which slows down the speed of the disc due to the friction between the disc and the pad. And finally, the disc stops [4]. One of the advantages of disc brakes compared to drum brakes is easier cooling, lighter weight, and easy placement. Fig. 1-a shows the components of a disc brake.

Brake discs are made of different materials, but the important point that gives an advantage to each of these alloys is to increase the thermal coefficient of the disc and reduce its depreciation against high contact and wear. Materials used in brake discs include stainless steel, gray cast iron, carbon ceramic composites, titanium alloys, and aluminum matrix composites. Ceramic composites have received much attention due to their high thermal and mechanical properties. These properties include thermal conductivity, mechanical strength, hardness, and high-temperature resistance. The improvement of their performance is due to the use of ceramic materials in the matrix and reinforcement, and ceramic composites are also used in various applications, including automotive brake discs. It should be noted that the way of processing and manufacturing

directly affects the properties of composites. Common manufacturing methods of ceramic composites include powder infiltration processing and slurry impregnation, polymer infiltration and thermal decomposition (PIP), chemical vapor infiltration (CVI), direct metal oxidation (DMO), and liquid silicon infiltration (LSI). Choosing the right method to produce a ceramic composite depends on various factors, such as the type of user, construction cost, and availability of raw materials, tools, and equipment [5].

Heydar Khalil et al. [6] analyzed the automotive disc brake. This article compared temperature distribution, deformation, and Von-Mises stress of gray cast iron and carbon ceramic brake discs. The results showed that carbon ceramic could show more resistance against thermal stress, and there is almost no deformation for it. In addition, carbon ceramic was preferred to achieve better brake performance. Venkatraman et al. [7] investigated and analyzed the brake disc using Ansys software. In this research work, they proposed the design of a disc brake with a copper lining, and its purpose was thermal analysis and temperature distribution in the brake disc. The results showed that the maximum heat produced in the brake disc made of gray cast iron without copper lining is 603.5 °C., while the maximum temperature produced in the brake disc with copper lining is 335.98 °C. Therefore, it is concluded that copper lining can be used in the brake disc at high temperatures.

Manavlan et al. [8] analyzed gray cast iron and ceramic brake disc using the finite element method in Ansys software. Their goal was to predict the temperature distribution in brake discs. This article used ceramic composites with carbon materials instead of traditional ceramic brake discs. The results showed that heat production decreases by adding carbon to ceramic materials because their thermal conductivity coefficient increases. Therefore, this increases the life of the brake and also improves its performance of the brake. Belhousin Ali [9] analyzed brake discs and automotive pads using the finite element method. This research aimed to study the thermodynamic behavior of automotive disc brakes in the braking phase and then a completely mechanical study of the dry contact between the disc and the pads. The results of this research showed that the tension on the surface of the disc increases during braking. In addition, the friction path between the disc and the pads, causes mechanical (radial) phenomena such as cracks, wear, and tears. Also, the presence of grooves in the pads adversely affects the brake's mechanical behavior. The important point here is that disc deformation increases significantly when thermal and mechanical stresses are combined.

Limpert [10] investigated the thermal characteristics of cast iron discs, which led to the rupture and cracking of the disc surface. Thermal stress analysis showed that disc surface rupture occurs when the induced compressive stress exceeds the compressive yield strength of a brake disc, which is an important factor that causes disc cracking during repeated braking. Soderberg et al. [11] investigated and analyzed the contact between the pad and the brake disc to determine the amount of wear with the help of Ansys software. In this research, they performed two wear simulations, one with disc displacement and the other without displacement. The approximate sliding distance is 75 meters, and the analysis solution time is three minutes. The analysis results showed that the deepest wear occurs in the high-pressure area; while there is almost no wear at the edge, after 1600 rotations, the wear process remains in a constant state, where all points on the surfaces have the same wear rate.

Mojavar et al. [12] investigated and thermally analyzed the automotive brake disc with the aim of temperature distribution in the disc during operation using Ansys software. The results of the thermal analysis showed that the temperature increases from 300 to 800°C during braking and also showed that the thermal conductivity of the brake pad material is smaller than that of the brake disc. In a study, Sridevi et al. [13] modelled and analyzed the structural and thermal disc brakes of the Honda Civic with three different materials, including steel, cast iron, and aluminium alloy, all of which are stainless. Because the real disc is without holes, they created holes in the design to dissipate more heat. Thermal analysis was performed by Ansys software. The results showed that the Von-Mises stress values of the disc with aluminum alloy are lower than steel and cast iron, and thermal analysis showed that the thermal gradient in the aluminum alloy is higher than in steel and cast iron, while the lowest thermal gradient was observed in steel. Pranta et al. [14] performed a computational study on modified disc brake rotors' structural and thermal behavior. They developed the disc brake rotor as a modified ventilated disc with curved cross-section valves with holes and slots. They analyzed the stress and temperature distribution using the finite element method with the help of Ansys software. They compared the results with the structural and thermal characteristics of the reference disc brake rotor. The analysis showed that the proposed disc brake rotors perform better than conventional disc brake rotors in terms of stress generation, temperature distribution, and safety factors.

Suval et al. [15], in their research, investigated the problems in Yamaha FZ_25 disc brakes. In this research, they presented four different models of the ventilated disc, the first model has equal and symmetrical holes, the second model has equal and asymmetrical holes, the third model has smooth and straight grooves, and the fourth model has curved grooves. They performed the analysis using the finite element method with the help of

Ansys software and compared the obtained results with the reference brake disc. The main goal of this research was to choose the best design to solve the problems in the reference disc and improve it, such as reducing the disc's weight, reducing the disc's deformation, and reducing the stress and temperature in the disc. The analysis results of four disc models indicate that the fourth model has managed to provide better performance than the original disc by increasing the stable stress by 2.05 MPa and reducing the deformation by 0.0002 mm. Also, this model performs better than the original disc and other models by increasing the stable temperature up to 15.73 °C, reducing the weight by 0.05 kg, and reducing the production cost by 9.26 rupees. In their research, Raj Kamal et al. [16] investigated and analyzed the structure of automotive disc brakes. The main goal of this research is to reduce the failure of the brake disc by using a material that has positive effects compared to the current brake disc manufacturing materials; that is why they replace the brake disc with materials including stainless steel, cast iron, and carbon-carbon composite in terms of deformability and thermally. They were analyzed using the finite element method to determine the temperature coefficient. The results obtained with the disc made of vanadium steel were investigated and compared. Completing this analysis proved that vanadium steel has better resistance and temperature distribution factors than the other three materials.

The innovation of ceramic brake discs and pads in automotives, compared to conventional brake discs and pads, is the reduction of brake dust, reduction of heat loss, reduction of noise, high durability and longevity, and corrosion resistance. Ceramic disc plates are easily able to perform their tasks at 800 °C, and this is thanks to the process of processing carbon fibers, and due to the low specific weight of the materials used, the amount of heat that is generated is less. Since such a structure is resistant to rust and erosion, its performance is at least 300,000 km. Also, ceramic discs have a 50% weight reduction compared to conventional metal discs, which significantly increases the automotive's controllability. The conducted studies show that little research has been done in the field of finite element analysis of ceramic disc type; Therefore, in this research, finite element analysis is performed on Peugeot 206 brake disc and pad by defining the characteristics of two types of ceramic and cast iron and comparing them in dynamic-thermal terms.

2 MATERIALS AND METHODS

2.1. Materials Used to Make Discs and Pads

This research uses materials such as gray cast iron and ceramic composites to make the brake disc. In this research, ceramic composite is considered for making brake discs made of c/c/sic composites by liquid silicon infiltration method (LSI) and brake pads made of gray cast iron. The mechanical and thermal properties of the brake disc (composite c/c/sic) and brake pad (gray cast iron GG25), as well as the characteristics of the brake disc (cast iron), are presented in "Tables 1 and 2".

Table 1 Mechanical properties of brake disc and pad [17]

Specification	Pad (gray cast iron GG25)	Disc (ceramic composite c/c/sic)	Cast iron disc
Density kg/m^3	1400	1900	7250
Modulus of elasticity (E) Gpa	103	140	130
Porosity	--	0.3%	--
Poisson's ratio (ν)	0.25	0.34	0.28
Friction coefficient between disc and brake pads (μ)	0.35		

Table 2 Thermal properties of brake disc and pad [17]

Specification	Pad (gray cast iron GG25)	Disc (ceramic composite c/c/sic)	Cast iron disc
heat transfer coefficient k (w/m^2.^{o}C)	5	20	11
specific heat c (J/kg.^{o}C)	1000	1200	460
Thermal expansion coefficient α, 10^{-6}/^{o}C	10	5	8

2.2. Geometry and Dimensions of Brake Disc and Pad

The brake disc and pad dimensions were measured for 3D modeling in Catia software by calipers ("Fig. 2"), and the radius and thickness of the disc and pad were measured as input for finite element analysis in Abaqus software. Figures 3 and 4 show the Peugeot 206 brake disc and caliper and the measured brake disc and pad symbols, respectively. The measured dimensions can be seen in "Table 3".

Fig. 2 Measurement of Peugeot 206 brake disc by caliper.

Fig. 3 Peugeot 206 brake disc and caliper.

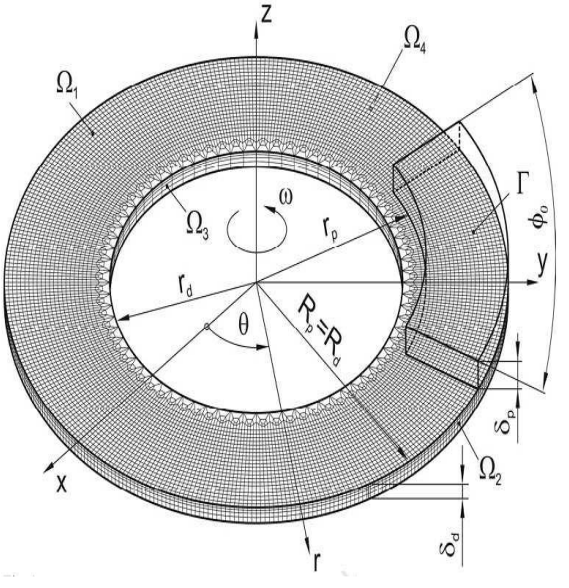

Fig. 4 Measured brake disc and pad symbols.

Table 3 Measured dimensions of brake disc and pad

Dimensions	Concept	Symbol
91 mm	Brake pad inner radius (mm)	r_p
133 mm	The outer radius of the brake pad (mm)	R_p
78 mm	Brake disc inner radius (mm)	r_d
133 mm	The outer radius of the brake disc (mm)	R_d
6.70 mm	Brake disc thickness (mm)	δ_d
13.6 mm	Brake pad thickness (mm)	δ_p

2.3. Brake Disc and Pad Modeling

A three-dimensional brake disc and pad model was modeled for dynamic analysis using Catia software ("Fig. 5").

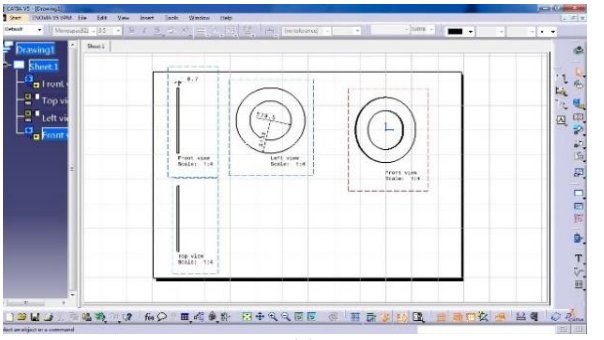

(a)

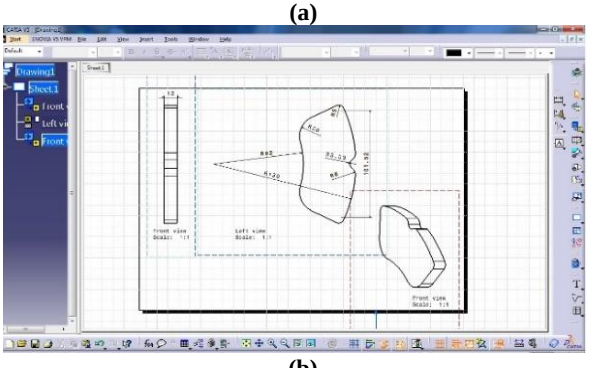

(b)

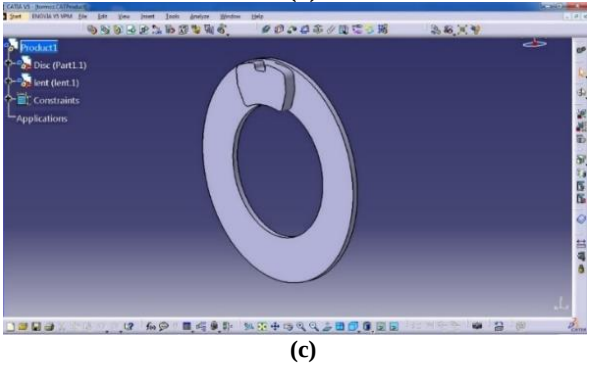

(c)

Fig. 5 Modeling of Peugeot 206 brake disc and pad in Catia: (a): Disc map, (b): Pad map, and (c): 3D model of disc and pad.

2.4. Dynamic-Thermal Analysis and Safety Factor Calculation

The main goal of this research is the thermomechanical analysis and investigation of temperature and pressure distribution between pads and discs in disc brakes. Therefore, the goal is to obtain a suitable model to identify hot spots between them through simulation to optimize and upgrade the disc brake system.

2.4.1. Dynamic Analysis

In inelastic stress analysis, a mathematical Equation includes three main stresses known as the yield function. If the calculated yield function is greater than the initial value, yield strength of the material, plastic strain, and softening or hardening will occur. In general, there are several yield functions to investigate the state of stress beyond the elastic region, including the Von-Mises stress criterion and the maximum shear stress. If a

material is subjected to pressure beyond that, a change in the yield surface occurs in the elastic region. There are two basic types of change in the yield surface. One is based on the assumption that the center of the yield surface remains constant while, at the same time, the yield surface expands without deformation, known as isotropic hardening. The other, known as kinematic hardening, is based on the assumption that the yield surface is visible in the stress space but does not change its size or shape. Both shear stress and Von-Mises stress are criteria used to predict the yield levels of flexible materials.

In contrast, the maximum normal stress criterion is usually used to predict the failure of brittle materials because the yield stress occurs at low strain levels and is difficult to define. Shear and Von-Mises stress are generally used when structural materials are flexible. Von-Mises theory predicts failure more accurately, but Tresca theory is often used in the design because it is simple and more consistent. Von-Mises theory relates the distortion energy of a point under the general state of stress. A state of hydrostatic stress occurs when all three main stresses are equal. In this condition, normal strains are equal in all directions, and there is no shear stress due to symmetry.

2.4.2. Thermal Analysis

When an automotive is moving at speed, it has kinetic energy. By applying the brakes, the pads pressing on the brake disc convert this energy into thermal energy. All of this is related to the first law of thermodynamics, known as the law of conservation of energy, which states that energy is neither created nor destroyed but is transformed from one form to another. In the case of brakes, it is converted from kinetic energy to thermal energy; which is equal to:

$$E_c = {}^1\!/_2\, m{V_0}^2 \tag{1}$$

In Equation 1, m is the automotive's total mass, and V_0 is its initial speed. To obtain the amount of heat released by each brake, one must extract the automotive's weight distribution. Therefore, the amount of heat released from each disc is equal to the following:

$$Q = 0.5 \times {}^1\!/_2\, m{V_0}^2 = 0.25\, {V_0}^2 \tag{2}$$

The heat energy generated by brake friction can be transferred to the brake disc and pads. This distribution of thermal energy depends on the relative thermal resistances of the pad and brake disc, which is a function of the density of the respective materials, their thermal capacities and thermal conductivity, as well as the presence of any transfer film or third layer of the body at the interface. In theory, the thermal resistance of the pad should be higher than the thermal resistance of the disc to protect the brake fluid from high temperatures. Still, the amount of thermal resistance varies from one pad material to another. In this analysis, the following relations and calculations are performed to calculate the heat distribution coefficient between pad and disc (γ) for thermal input to the brake disc. The thermal penetration of the disc ξd and the thermal penetration of the pad ξp are obtained from the following relationships [17]:

$$\xi_d = \sqrt{K\rho_d c_d} \tag{3}$$

$$\xi_p = \sqrt{K\rho_p c_p} \tag{4}$$

Where, K is the heat transfer coefficient, ρ is the density, and c is the specific heat of the disc and pad. Sd and Sp, which are the disc and pad frictional contact surfaces, respectively, are obtained from the following relations:

$$S_d = 2\pi \int_{r_2}^{r_3} r dr \tag{5}$$

$$S_p = \varphi_0 \int_{r_2}^{r_3} r dr \tag{6}$$

Where, φ_0 is the central angle of the pad and r_2, and r_3 are the internal and external radii of the disc, respectively ("Fig. 6").

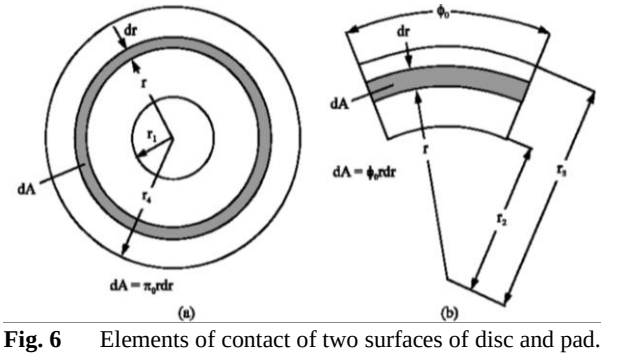

Fig. 6 Elements of contact of two surfaces of disc and pad.

The relative braking energy (γ), which is called the heat distribution coefficient, is obtained by the following Equation:

$$\gamma = \frac{\xi_d S_d}{\xi_d S_d + \xi_p S_p} \tag{7}$$

The ratio of heat generated for friction between this surface is calculated from the following Equation:

$$d\dot{E} = r\omega\mu p\varphi_0 r dr \tag{8}$$

Where, φ_0 is the central angle of the pad, μ is the friction coefficient, ω is the angular velocity, and p is the surface contact pressure.

The heat flux in the disc for uniform pressure is a function of time and the change of the distance r, the reduction of the angular velocity during the braking time, and the work done by the friction force. This phenomenon often happens when the pads are new. The heat flux in the disc is obtained from the Equations (9-a and b) [17]:

$$q_d(r,t) = \frac{d\dot{E}_d}{dS_d} = \frac{\gamma\omega\mu p\varphi_0 r^2 dr}{2\pi r dr} = \frac{\varphi_0}{2\pi}\gamma\mu p r\omega_t \qquad (9\text{-a})$$

$$q_{0d}(r,0) = \frac{d\dot{E}_d}{dS_d} = \frac{\gamma\omega\mu p\varphi_0 r^2 dr}{2\pi r dr} = \frac{\varphi_0}{2\pi}\gamma\mu p r\omega_0 \qquad (9\text{-b})$$

Where, γ is the heat distribution coefficient between the pad and disc, φ_0 is the central angle of the pad, μ is the friction coefficient, ω is the angular velocity, dE˙ is the rate of heat produced due to friction between two surfaces and r is the radius of the disc.
The heat flux in the pad is also obtained from the Equations (10-a and b):

$$q_p(r,t) = \frac{d\dot{E}_p}{dS_p} = \frac{(1-\gamma)\omega\mu p\varphi_0 r^2 dr}{\varphi_0 r dr} = (1-\gamma)\mu p r\omega_t \qquad (10\text{-a})$$

$$q_{0p}(r,0) = \frac{d\dot{E}_p}{dS_p} = \frac{(1-\gamma)\omega\mu p\varphi_0 r^2 dr}{\varphi_0 r dr} = (1-\gamma)\mu p r\omega_0 \qquad (10\text{-b})$$

2.4.3. Calculation of Safety Factor

The conventional design method in mechanical engineering, which is sometimes called the classical method or deterministic design method, is based on the concept of the safety factor. This means that the design of different parts is done in such a way that the maximum applied stress is smaller than the minimum resistance of the materials used in the structure or part. In this research, the safety factor was determined using the theory of energy and torsion. According to the DE theory, material destruction due to yielding occurs when the torsional strain energy (or distortion energy) per unit volume is equal to or greater than the strain energy, such as its tensile or compressive yield strength. The theory of torsional energy is widely used in the case of deformable materials, and this theory should be used in problems where the type of theory is not mentioned [18]. In the DE theory, the Von-Mises stress component is calculated from Equation (11):

$$\sigma' = \left[\frac{(\sigma_1-\sigma_2)^2+(\sigma_2-\sigma_3)^2+(\sigma_3-\sigma_1)^2}{2}\right]^{1/2} \qquad (11)$$

Where, σ_1, σ_2 and σ_3 are the main stresses in the part and σ' is the component of Von-Mises stress. The safety factor is also determined from Equation (12):

$$\sigma' = \frac{S_y}{n} \qquad (12)$$

In this relation, S_y is the yield strength of the material used in the construction of the part and n is its safety factor.
Since the elastic stresses and strains are fully reversible and non-cumulative, the brake disc model is only considered for one braking period. The range of elastic strain with the range of stress σ_a is by Hooke's law in the form of Equation (13):

$$\varepsilon_e = \frac{\sigma_a}{E} \qquad (13)$$

Where, σ_a is stress, ε_e is elastic strain and E is modulus of elasticity.

2.5. Dynamic and Thermal Analysis of Finite Element Using Abaqus Software

After 3D modeling of disc and brake pad in Catia software; for dynamic analysis using the finite element method, the 3D model was transferred to Abaqus software.

2.5.1. Determining the Properties of Ingredients in The Property Module

The mechanical properties of ceramic and gray cast iron were defined for disc and brake pad, respectively, according to "Table 1" in the property module of the Abaqus program, which included density, Poisson's ratio, thermal conductivity coefficient, specific heat, and modulus of elasticity ("Fig. 7").

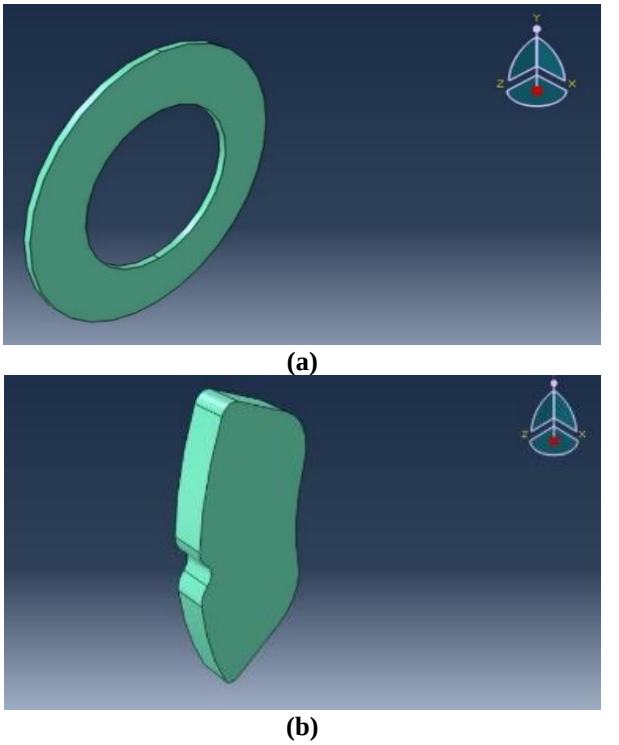

(a) **(b)**

Fig. 7 (a): Determining the properties of disc materials, and (b): Determining the properties of brake pad materials.

2.5.2. Assembling the Disc and Pad

Each model in Abaqus may consist of different parts, which are used to put these parts together and form a final system and apply geometric constraints between them using the Assembly module. This module's disc and brake pads form an integrated brake system after assembly ("Fig. 8"). Since each of these parts is designed in the same coordinates, when they are called in this part, they may overlap with each other, so to move them, the option Translate instance is used to move the vector.

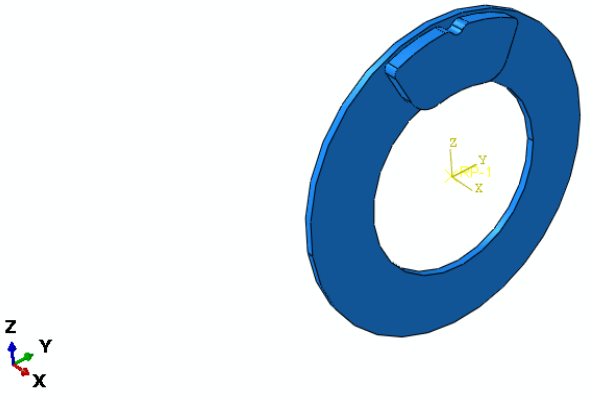

Fig. 8 Disc and pad assembly.

2.5.3. Problem-Solving and the Type of Analysis in The Step Module

Each physical phenomenon has its differential Equations. Due to the dynamic nature of brake disc and pad analysis, a suitable solver is used to analyze the heat of folding from the friction between the disc and the brake pad. For this purpose, the Dynamic Explicit option, i.e., dynamic analysis with a braking time of 4 seconds, is considered in the Step module. Also, the purpose of doing a project in Abaqus software is to get a series of output data and analyze and check them. For this purpose, it is determined in the Step module that at the end of the work, dynamic stresses are delivered as output.

2.2.4. Contact Between the Disc and The Pad in The Interaction Module

Undoubtedly, the importance of collision and contact for analyzing a set in Abaqus is very high; therefore, in this study, we must specify the type of contact between the pads and the brake disc in the Interaction module ("Fig. 9"). Also, in this section, the contribution of the heat input to the disc and pad during braking should be determined, which is calculated using Equation (14). After calculating it, you should enter the obtained numbers in the Interaction module:

$$\frac{Q_d}{Q_p} = \frac{\sqrt{\rho_{d*}\lambda_{d*}c_d}}{\sqrt{\rho_{p*}\lambda_{p*}c_p}} \qquad (14)$$

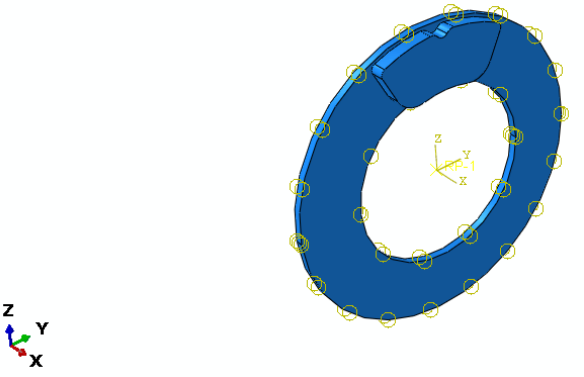

Fig. 9 Determination of the type of disc and pad contact.

Where, Q_d is the heat input to the disc, Q_p is the heat input to the pad, ρ is the density, λ is the heat transfer coefficient, and c is the specific heat capacity.

2.5.5. Boundary Conditions and Application of Forces in The Load Module

In this section, the initial temperature of the disc and pad is assumed to be 30 °C, at time t=0, while the constant heat flux produced by pressing the pad on the friction surface of the disc is the only input heat source of the model. The boundary conditions in the symmetry state for the disc should only have rotation around the X axis (U_1) and no rotation along the Y and Z axes. It should also specify the same stages of boundary conditions for the pad that has freedom of movement only in the direction of the X-axis. The initial speed of the disc in this section should be specified as VR1, i.e., the speed around the X-axis, which is 260 radians/second here. The force applied to the pad during braking is a compressive force equal to one MPa. ("Fig. 10").

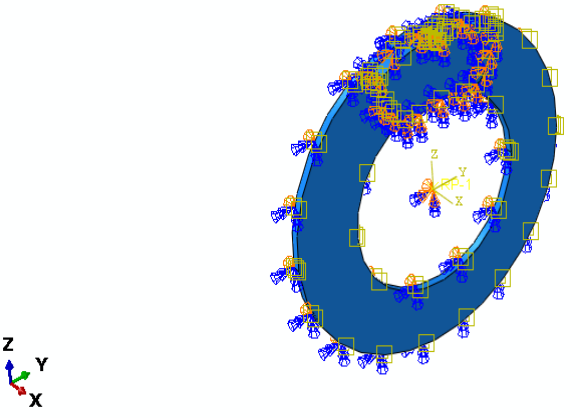

Fig. 10 Determination of the boundary conditions and applying force on the disc and pad.

2-5-6- Meshing and Loading Conditions of Disc and Pad

In this research, the elements used for meshing, due to the symmetry of half of the disc and one number of brake pads, hexahedral (C3D8T) meshing with eight nodes, was used and created a regular network of elements in it. ("Figs. 11 and 12"). The number and size of the elements are inversely proportional to each other; that is, the more the number of elements in the mesh created on geometry, the smaller the size of the elements [19]. According to "Fig. 13", with the increase in the number of elements (the elements become smaller), the stress has converged to a fixed limit.

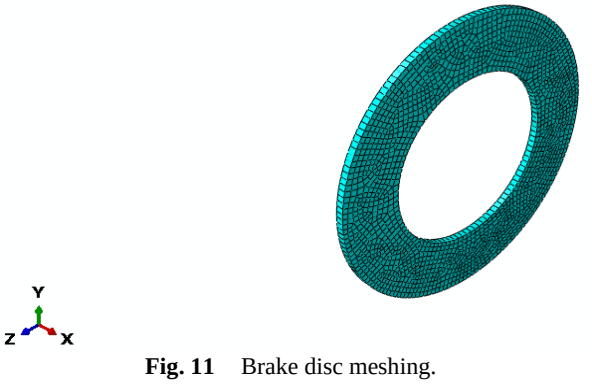

Fig. 11 Brake disc meshing.

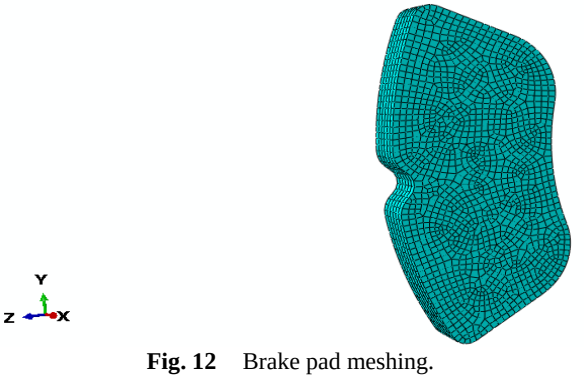

Fig. 12 Brake pad meshing.

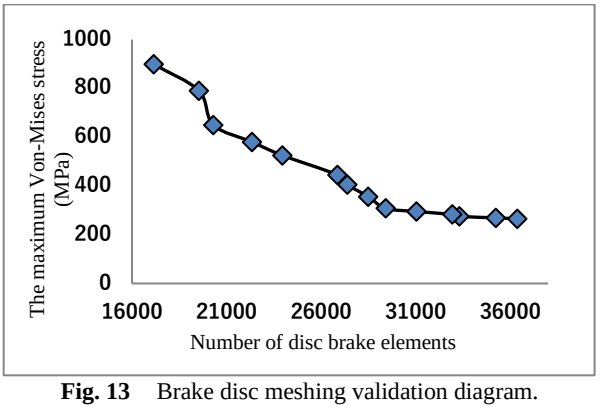

Fig. 13 Brake disc meshing validation diagram.

3 RESULTS AND DISCUSSION

3.1. Von-Mises Stress of Disc

Figure 14 shows the Von-Mises stress contour of the ceramic disc. According to this Figure, the maximum Von-Mises stress in the contact area between the pad and the disc is equal to 260.7 MPa; meanwhile, in the cast iron disc ("Fig. 15"), the maximum Von-Mises stress is equal to 293.3 MPa. Figure 16 also shows the Von-Mises stress contour of an element of a ceramic disc.

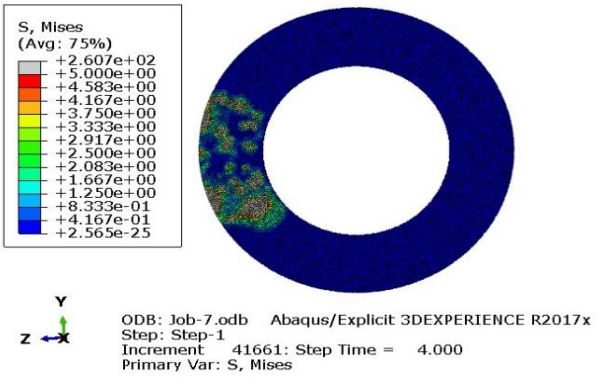

Fig. 14 Von-Mises stress contour of ceramic disc.

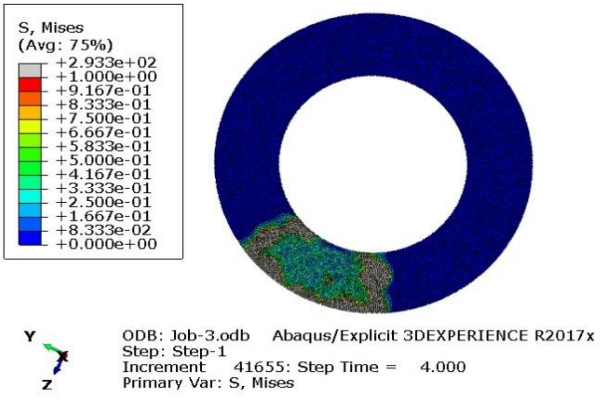

Fig. 15 Von-Mises contour tension of cast iron disc.

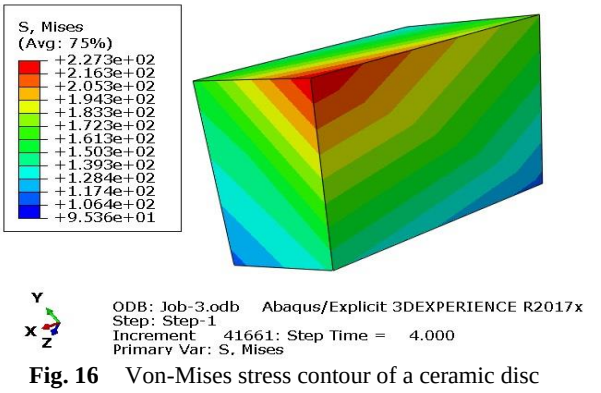

Fig. 16 Von-Mises stress contour of a ceramic disc element.

3.1.1 Von-Mises Stress in The Peripheral Path of The Disc

This analysis analyzed three different paths of Von-Mises stress on the surface of ceramic and cast iron discs. Figure 17 shows a path marked on the surface of the ceramic disc and close to the hub for the Von-Mises stress.

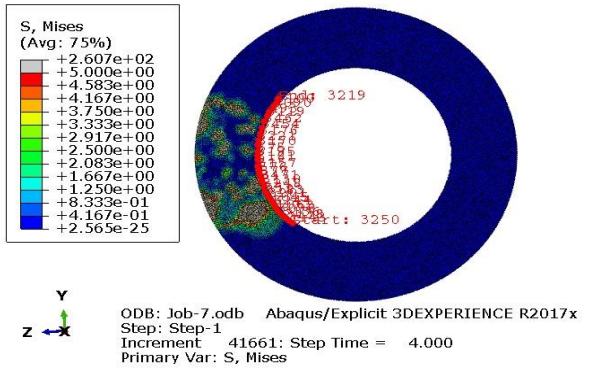

Fig. 17 Von-Mises stress of the path on the surface of the inner diameter of the ceramic disc.

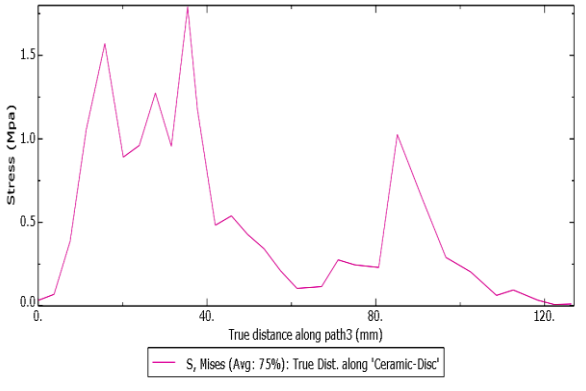

Fig. 18 Von-Mises stress diagram of the path on the surface of the inner diameter of the ceramic disc.

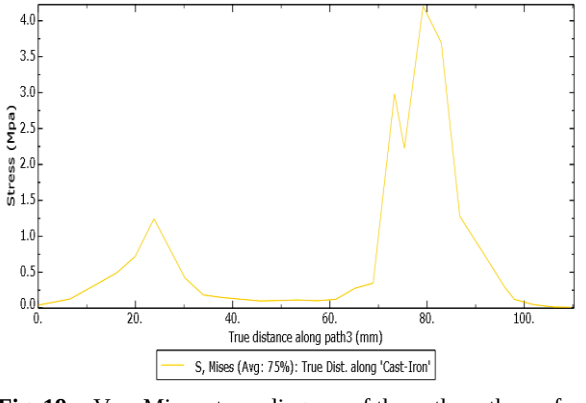

Fig. 19 Von-Mises stress diagram of the path on the surface of the inner diameter of the cast iron disc.

The Von-Mises stress diagram related to this path ("Fig. 18") shows that the Von-Mises stress in the ceramic disc is between 0 and 1.75 MPa, while the value of Von-Mises stress in the same direction on the surface of the cast iron disc ("Fig. 19") fluctuates between 0 and 4 MPa.

3.1.2. Von-Mises Stress in The Disc Thickness

Figure 20 shows the Von-Mises stress diagram in the thickness of the ceramic disc. According to this figure, the stress is linear, and from the beginning of the path to the thickness of 2.3 mm, its value is nearly 20 MPa, and after that, this stress increases until the end, and its value reaches 75 MPa. Compared to the Von-Mises stress diagram in the thickness of the cast iron disc ("Fig. 21"), the stress along the path of the disc thickness increases from the beginning and reaches 14.5 MPa.

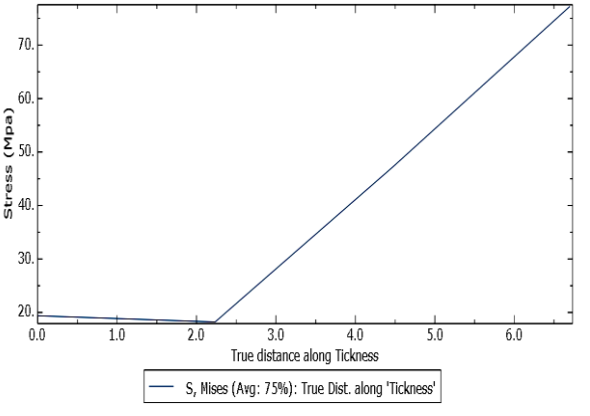

Fig. 20 Von-Mises stress diagram in the thickness of the ceramic disc.

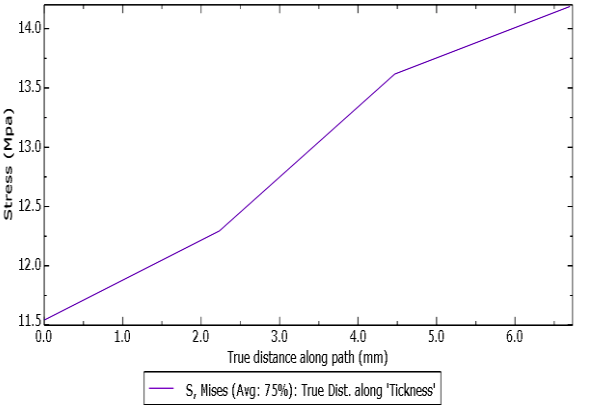

Fig. 21 Von Mises stress diagram in the thickness of cast iron disc.

3.1.3. Comparison of Safety Factor of The Ceramic Disc and Cast-Iron Disc

It was considered that the yield strength of the ceramic disc is 498 MPa, and the yield stress of the cast iron disc

is 425 MPa. Therefore, by placing these numbers and the maximum Von-Mises stress value obtained from the finite element analysis in Equation (12) and solving it, the coefficient Confidence is calculated. Comparing the safety factor values of the ceramic and cast iron disc shows that the ceramic disc has a higher safety factor ("Table 4").

Table 4 Safety factor of ceramic and cast-iron disc

Safety factor of ceramic disc	Safety factor of cast iron disc
1.98	1.45

3.1.4. Shear Stress in Ceramic Disc

The shear stress contour (τ_{xy}) is shown in "Fig. 22". The lowest shear stress in the xy direction equals -25.62 MPa, and the highest shear stress in the xy direction is +42.01 MPa. Also, the shear stress contour (τ_{xz}) is shown in "Fig. 23". The lowest shear stress in the xz direction equals -36.97 MPa, and the highest stress in the xz direction is +99 MPa. "Table 5" compares shear stress values in ceramic and cast-iron discs.

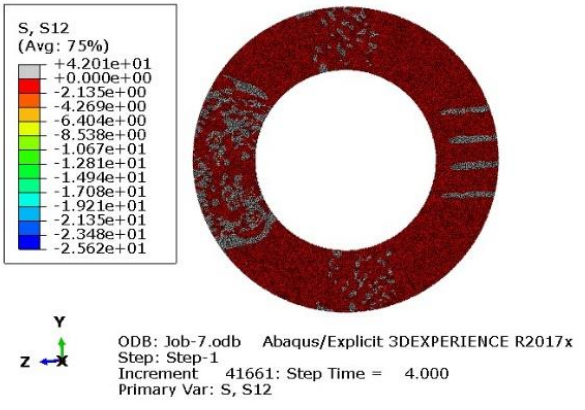

Fig. 22 Shear stress contour (τ_{xy}) in ceramic disc.

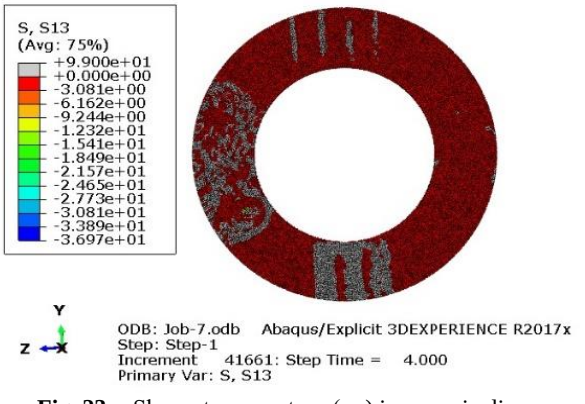

Fig. 23 Shear stress contour (τ_{xz}) in ceramic disc.

Table 5 Comparison of shear stress values in ceramic and cast-iron discs

shear stress	The lowest shear stress (MPa)		The highest shear stress (MPa)	
	cast iron disc	Ceramic disc,	cast iron disc	Ceramic disc,
τ_{xy} (S12)	-43.27	-25.62	+44.45	+42.01
τ_{xz} (S13)	-43.87	-36.97	+130.5	+99
τ_{yz} (S23)	-80.15	-79.53	+90.04	+70.78

3.1.5. Movement in Ceramic Disc

The displacement contour in Fig. 24 shows that the amount of displacement after the braking action is between 0 and +0.00002 mm.

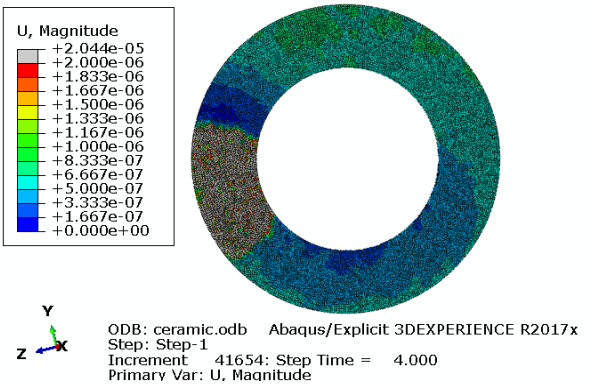

Fig. 24 Displacement contour in ceramic disc.

2.3. Estimating the Temperature on The Surface of The Ceramic Disc and Comparing It with The Cast Iron Disc

Figure 25 shows the surface temperature contour of the ceramic disc, which is predicted by the finite element method by Abaqus software at the end of the braking operation for 4 seconds.

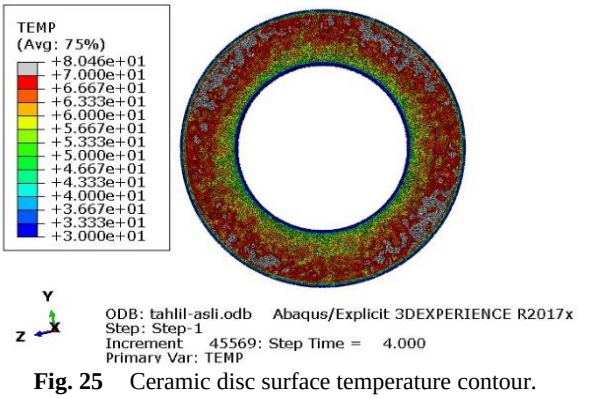

Fig. 25 Ceramic disc surface temperature contour.

As can be seen, the maximum surface temperature of the ceramic disc is 80.46 °C, which is 148.1 °C, which is 84% lower than the cast iron discs ("Fig. 26"). Therefore, it can play a significant role in braking performance and ability. This analysis considers gray cast iron brake pads for both ceramic and cast iron discs.

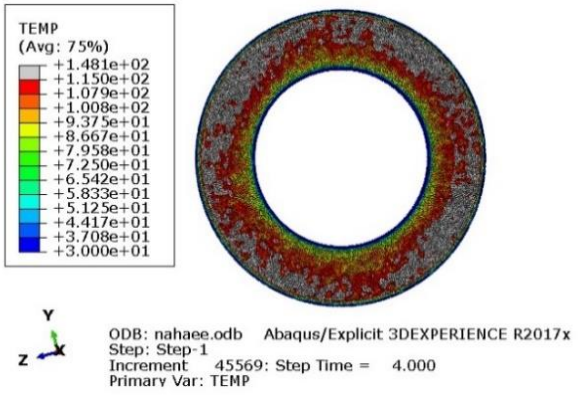

Fig. 26 Cast iron disc surface temperature contour.

Figure 27 shows the contour of an element of a ceramic disc where the highest temperature is on its surface. Also, Fig. 28 shows the temperature versus time graph that shows a sudden increase in temperature from the initial moment of braking to the first second. In another 3 seconds from the time of full braking, the temperature is in the maximum range due to the equal rate of heat generation and heat exit from the contact area.

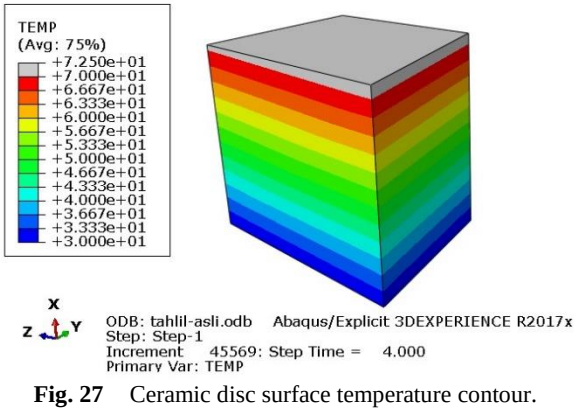

Fig. 27 Ceramic disc surface temperature contour. Temperature contour of a ceramic disc element.

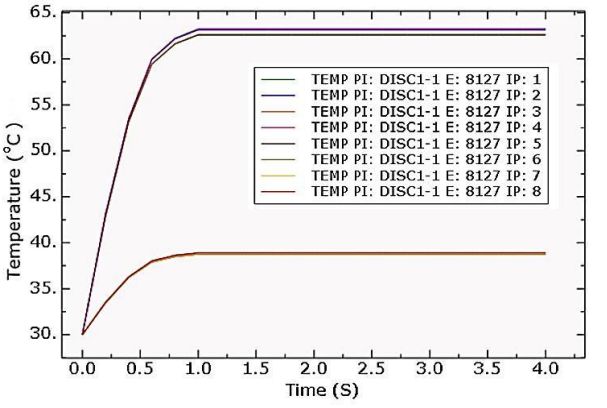

Fig. 28 Ceramic disc surface temperature contour. Temperature-time diagram of an element of ceramic disc.

3.2.1. Temperature Distribution in The Peripheral Path of The Ceramic Disc

This analysis analyzed three environmental paths (external, middle, and internal) of the surface of the ceramic disc. Figure 29 shows the temperature contour in the second path (average environment) as an example. The temperature distribution diagram related to this path in "Fig. 30" shows that the temperature distribution in this path is mainly in the temperature range between 65 and 75 °C. Compared to the temperature distribution in the same route on the surface of the cast iron disc ("Fig. 31"), the temperature is mainly in the range between 100 and 130 °C.

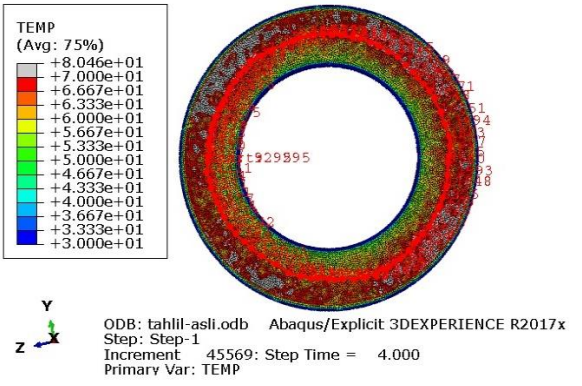

Fig. 29 Ceramic disc surface temperature contour. Temperature distribution (average path) on the ceramic disc surface.

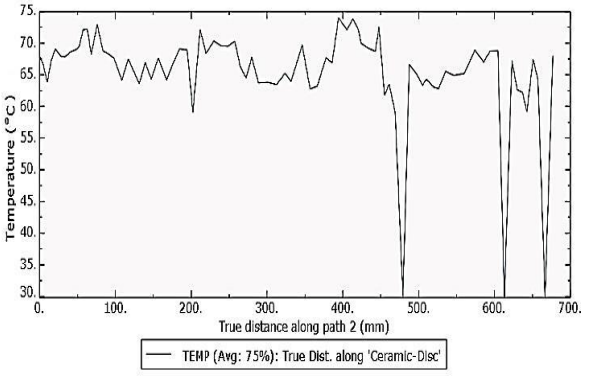

Fig. 30 Ceramic disc surface temperature contour. Temperature distribution diagram in the medium path (ceramic disc).

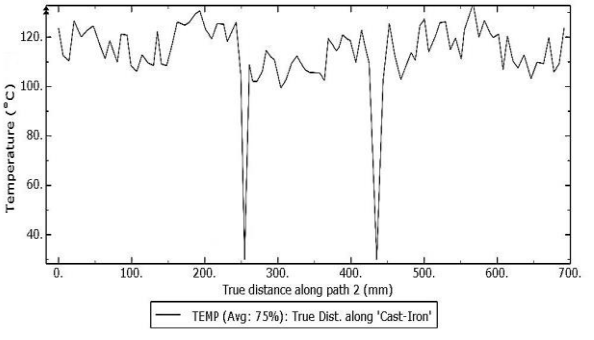

Fig. 31 Ceramic disc surface temperature contour. Temperature distribution diagram (average path) of cast iron disc.

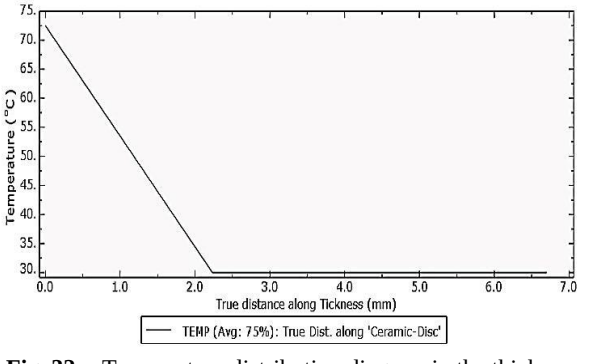

Fig. 32 Temperature distribution diagram in the thickness of the ceramic disc.

3.2.2. Temperature Distribution in The Thickness of The Ceramic Disc

As “Fig.32” shows, the temperature distribution in the disc's thickness started from the pad's surface and the disc with a temperature of 72.5 °C. It penetrated to a depth of 2 mm from the disc's thickness. The rest of the way, the temperature of the disc thickness remains constant in the ambient temperature range; this is due to the contact of the back surface of the disc with air and its cooling.

3.2.3. The Effect of Temperature on The Reduction of Braking and Friction Coefficient

Brake discs are forced to absorb a significant amount of heat during braking. Decreasing braking creates a situation where heat is generated faster than it can transfer to the surrounding environment. The normal temperature of the disc in everyday driving is less than 135°C; during frequent braking, excessive heat may be generated, which reduces the brake's ability and even breaks it down. High temperature in disc brakes reduces the coefficient of friction and thus reduces friction, and high temperature also increases wear. The same things mentioned affect the performance of disc brakes and reduce the amount of braking power. Considering that the maximum temperature produced in the ceramic disc is 80.46°C (“Fig. 25”), it is concluded that even in frequent braking, the temperature of the ceramic disc is lower than usual. It shows that the ceramic disc does not lose its ability in regular braking.

3.2.4. The Effect of Temperature on The Formation of Tribo Layer, Wear, And Cracking

Pad and disc surfaces change their characteristics due to friction, wear, and other mechanical interactions related to increased frequent braking and increased temperature. The temperature created in the contact between the pad and the disc is a significant influencing factor on friction. It can be explained from the perspective that temperature affects the formation of the so-called tribo layer. Surfactant additives are present in the contact line of the pad and disc contact surfaces and control friction. The speed of production of this layer is influenced by surface activity dependent on temperature. Due to thermomechanical stresses caused by interactions resulting from friction, the ingredients of the disc and pad are gradually removed from its surface (wear occurs). Since the wear on the contact surface is high, the brake assembly's risk of failure and inefficiency increases. One of the explanations for this phenomenon is that metal wear debris fills the open area on the disc surface and increases the tendency for more friction between the two contact surfaces. It makes it easier for the two contacting surfaces to form an adhesive-like bond (welded joint).

The increase in disc temperature and the resulting thermal stress is the main cause of disc cracking, especially on the disc surface. This cracking can be caused by the thermal energy entering the friction surfaces. The occurrence of surface tearing and cracking that occurs in a brake depends on the induced temperature. During repeated braking, fatigue characteristics can be an important factor in determining the initiation of the disc cracking. The result of the analysis of the ceramic disc shows that due to the low temperature, wear, and cracking factors do not occur due to the high temperature.

4 CONCLUSIONS

This research used finite element analysis to study stress and temperature in ceramic disc brakes. By comparing the analysis of stress and temperature in ceramic discs compared to cast iron discs, the following results were obtained.

• The maximum Von-Mises stress in the ceramic disc is 260.7 MPa. This maximum tension is created in the contact area between the pad and the disc. While the maximum Von-Mises stress in the cast iron disc is 293.3 MPa.

• Comparison of shear stress values in ceramic and cast iron discs shows that cast iron disc has more shear stress in xy, xz and yz directions (respectively +44.45, +130.5 and +90.04 MPa) than ceramic disc. It is entered in xy, xz and yz directions (+42.01, +99 and +70.78 MPa, respectively).

• The comparison of calculated safety factor values of ceramic and cast iron disc showed that ceramic disc has a higher safety factor (1.98) than cast iron disc (1.45).

• Comparison of analysis of ceramic and cast iron brake discs during braking by finite element method showed that the amount of heat produced in the ceramic disc during braking action in 4 seconds is almost 84% less than the cast iron disc in the same period.

• The low temperature in the ceramic disc reduces wear and cracking and ultimately improves the braking performance of the brake disc.

REFERENCES

[1] Amrollahi Beyuki, H., Mahmoudi Kleiber, M., Chassis and Body Technology, In Persian, SAD Publications, 2019.

[2] Turner, W.V., The Air Brake as Related to Progress in Locomotion. Pittsburg, Pennsylvania: Westinghouse Air Brake Company, 1910.

[3] Buckman, L. C., Commercial Vehicle Braking Systems: Air Brakes, ABS and Beyond, Society of Automotive Engineers, Indianapolis, The 43rd L. Ray Buckendale Lecture, International Truck and Bus Meeting and Exposition, Indianapolis, Society of Automotive Engineers, 1998.

[4] Sowjanya, K., Suresh, S., Structural Analysis of Disc Brake Rotor, International Journal of Computer Trends and Technology (IJCTT), Vol. 4, No. 7, 2013.

[5] Jahdi, R., Shakiba Jahormi, S., A Study on The Production and Application of Ceramic Matrix Composites in Macro and Micro Scale, In Persian, The First National Conference on Fundamental Research in Mechanical Engineering, Tehran, 2017.

[6] Khaleel, H. H., Khashan, M. K., and Baqir, A. SH., Modeling and Analysis of Disc Brake in Automobiles, Journal of Mechanical Engineering Research & Developments (JMERD), 2018.

[7] Venkatramanan, R., Kumaragurubaran, S. B., Vishnu Kumar, C., Sivakumar, S., and Saravanan, B., Design and Analysis of Disc Brake Rotor, International Journal of Applied Engineering Research, ISSN: 0973-4562, Vol. 10, No. 19, 2015.

[8] Manavalan, S., Aswin Gopi, J., Arivarasu, A., and Abishek, A. HI., Chandru, S., Review on Ceramic Disc Brake System, International Journal of Recent Technology and Engineering (IJRTE), ISSN: 2277-3878, Vol. 7, No, 6S2, 2019.

[9] Belhocine. A., Finite Element Analysis of Automotive Disc Brake and Pad in Frictional Model Contact, International Journal of Manufacturing, Materials, and Mechanical Engineering, Vol. 5, No. 4, 2015, pp. 32-62.

[10] Limpert, R., An Investigation of Thermal Conditions Leading to Surface Rupture of Cast Iron Rotors, SAE Technical Paper Series, , 1972, 720447.

[11] Söderberg, A., Andersson, S., Simulation of Wear and Contact Pressure Distribution at The Pad-To-Rotor Interface in A Disc Brake Using General Purpose Finite Element Analysis Software, International Journal of Wear, 2009.

[12] Mujawar, L., Savatekar, P., Korade, A., Naidu, A., Ekal, O., and Nalawade, S., Design and Thermal analysis of Disc Brake, International Research Journal of Engineering and Technology (IRJET), Vol. 05, No. 08, 2018.

[13] Sreedevi, K. N. V., Radha Krisha Prasad, P., Murali Krishna, M. V. S., and Gangireddy, J. N., Modeling and Analysis of a Disc Brake, International Journal of Science and Research (IJSR), ISSN: 2319-7064, 2018.

[14] Pranta, M. H., Rabbi, M. S., Banik, M. C., Hafez, M. G., and Ming Chu, Y. U., A Computational Study on Structural and Thermal Behavior of Modified Disc Brake Rotors, Alexandria Engineering Journal, 2022.

[15] Suwal, B., Maharjan, S., Design of Rotor Disc Brake using Structural & Thermal Analysis, IOE Graduate Conference, 2021.

[16] Rajkamal, M. D., Dylan Abraham Samson, T., Dhinesh Kumar, P., and Chithambaravishnu, S., Structural Analysis of Disc Brake, International Journal of Mechanical Engineering and Technology (IJMET), Vol. 9, No. 3, 2018.

[17] Deressa, K. T., Tilahun, D., Thermal Stress Analysis of Disc Brake Rotor by Finite Element Method, A Thesis Submitted to the Graduate School of Addis Ababa University in Mechanical Engineering, 2013.

[18] Budynas, R. G., Nisbett, J. K., Shigley's Mechanical Engineering Design (8th ed), McGraw-Hill's, 2008.

[19] Nazemosadat, S. M. R., Ghanbarian, D., Naderi-Boldaji, M., and Nematollahi, M. A., Structural Analysis of a Mounted Mouldboard Plough using Finite Element Simulation Method, Spanish Journal of Agricultural Research, Vol. 20 No. 2, 2022, pp. 1-14, https://doi.org/10.5424/sjar/2022202-18157.